Unified Crystallographic, Langmuir Layer, and Langmuir−Blodgett Film Investigation of Novel Amphiphiles Based on 4-Nitroaniline

Sonika Sharma and T. P. Radhakrishnan*

School of Chemistry, University of Hyderabad, Hyderabad − 500 046, India

Received: May 14, 2002; In Final Form: October 4, 2002

Crystal structures of amphiphilic molecules should serve as a convenient basis to explore the molecular associations and intermolecular interactions in the corresponding Langmuir layers and Langmuir−Blodgett (LB) films. However, the difficulty of growing single crystals of such molecules often precludes such investigations. We present, in this paper, the crystal structure investigation and LB film study of new amphiphiles based on the 4-nitroaniline moiety of interest in quadratic nonlinear optical applications. A molecular-level explanation of the general instability of monolayers of these amphiphiles is proposed based on near neighbor interactions observed in the crystals. An approach to stabilize them through the formation of composite bilayers with the phospholipid molecule, distearoylphosphatidylcholine (DSPC), is developed. The complex pressure−area isotherms of the composites and their transformation through multiple isocycles are interpreted using the molecular structure and conformation from single crystal analysis. Electronic absorption spectroscopy of the solution, solid state, and LB films complemented by semiempirical quantum chemical computations allows us to model the intermolecular interactions in the LB film. This study demonstrates a novel approach to correlating the 3-dimensional and quasi-2-dimensional assembly of molecules in crystals and Langmuir/LB films.

Introduction

One of the versatile aspects of molecular materials is the variety of forms in which they can be assembled, ranging from single crystals to amorphous powders, Langmuir−Blodgett (LB) films to thermally evaporated films, and host−guest complexes to embeddings in polymer films. Understanding the nature of intermolecular interactions is critical for the effective design and utilization of molecular materials. Among the different bulk structures with varied application potential, a detailed atomic/molecular level description of the interactions between the building blocks is most conveniently obtained in single crystals in which atom positions can be determined unambiguously through X-ray diffraction analysis. However, among the different approaches to the assembly of molecular materials, the LB technique stands out as a simple, elegant, and efficient organization tool.[1] Molecular assembly at the air−water interface and LB film deposition can be tailored by careful control of a variety of parameters including subphase composition and conditions, substrate preparation and dipping protocols. However in the majority of cases of interest in materials applications, the very nature of the molecules which form LB films, i.e., their amphiphilic structure, hampers the formation of good quality single crystals precluding a structure determination. We have carried out a crystallographic database[2] survey of amphiphilic molecules having an *n*-tridecyl or longer *n*-alkyl chain and bearing any kind of π-conjugated chromophore ring unit; the cutoff of the tridecyl unit was chosen because 12-carbon and shorter chain systems usually do not form stable monolayers. Crystal structures have been reported for only 31 cases, and a search of the literature indicated that of these only one system was characterized in LB studies;[3] however, no detailed correlation of single crystal and LB film characteristics was presented. This exercise demonstrates the paucity of systems of interest in optical materials applications on which detailed crystal structure characterization and LB studies have been concurrently carried out. In this paper, we present a combined crystallographic and Langmuir/LB film investigation of two amphiphilic molecules of potential interest in nonlinear optical (NLO) applications.

The prototypical "push−pull" system for molecule-based quadratic NLO materials is the 4-nitroaniline moiety; some of the most successful materials such as *N*-(4-nitrophenyl)-*S*-prolinol (NPP)[4] and methyl-(2,4-dinitrophenyl)-aminopropanoate (MAP)[5] are based on this framework. Despite several other families of NLO chromophores developed over the years, this basic structural unit continues to be the focus of fundamental studies.[6] Unfortunately, successive attempts at LB film fabrication of several amphiphiles based on the 4-nitroaniline derivatives have met with limited success.[7] Although this combination of NLO chromophore and molecular assembly technique is a prominent and unique one, little is known about the basic cause of its failure. A molecular level insight into this problem can be gained through a combination of structural investigation of crystals of the amphiphile and monolayer studies together with the examination of some physical characteristics common to both states of assembly.

The present study addresses this question and explores approaches to stabilize monolayers of amphiphiles based on the 4-nitroaniline moiety and to deposit their LB film. Because many of the successful crystalline NLO molecular materials are based on chiral molecules, we have chosen to study three new molecules: *N*-(4-nitrophenyl)-3(*R*)-octadecyloxypyrrolidine (NP3OP), *N*-(4-nitrophenyl)-O-hexadecyl-*S*-prolinol (NPOHP), and *N*-(4-nitrophenyl)-O-octadecyl-*S*-prolinol (NPOOP); the latter two are NPP derivatives. Amphiphiles such as these rarely

* To whom correspondence should be addressed. E-mail: tprsc@uohyd.ernet.in. Fax: 91-40-3012460.

10.1021/jp0261105 CCC: $25.00
Published on Web 12/10/2002

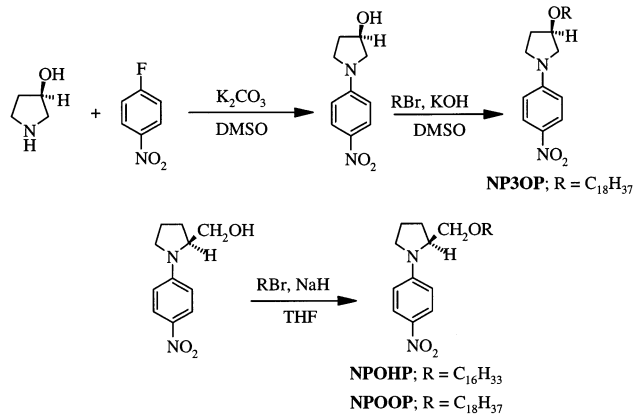

Figure 1. Scheme of synthesis of NP3OP, NPOHP and NPOOP.

form single crystals suitable for X-ray analysis. We have succeeded in growing crystals of NP3OP and NPOHP and have investigated their molecular structure and crystal packing. Similar to earlier observations on related systems,[7] these amphiphiles show very poor spreading behavior on water and do not form stable monolayers. We have stabilized them on the water surface by mixing with the phospholipid, distearoylphosphatidylcholine (DSPC). Characteristic features of the pressure−area isotherms of the composites are investigated in detail. Although pressure−area isotherms by themselves provide little structural information, together with the input from the crystal structures, we draw useful insight into the likely structure of the Langmuir layers. Finally, we have achieved quantitative transfer of the composite bilayers of NP3OP−DSPC and NPOOP−DSPC onto suitable substrates, and the deposited LB films are characterized using electronic absorption spectroscopy supported by semiempirical quantum chemical modeling. Correlation of the electronic absorption spectra of the crystalline material and the LB film allows us to extend the molecular level picture in the crystal to the LB film. The present study sheds light on intermolecular interactions that possibly impede stable monolayer formation of amphiphiles based on 4-nitroaniline and suggests routes for the fabrication of their LB films.

Experimental and Computational Section

Synthesis and Characterization. NP3OP, NPOHP, and NPOOP were synthesized following the reaction schemes in Figure 1. The products were characterized as follows:

NP3OP. mp = 82−84 °C. FT-IR (KBr): ν/cm^{-1} = 1520, 1483, 1331, 1105. ^{1}H NMR ($CDCl_3$) : δ/ppm = 8.1 (2H, d), 6.5 (2H, d), 4.2 (1H, broad), 3.2−3.6 (6H, m), 2.1 (2H, m), 1.5−1.6 (2H, m), 1.3 (30H, br s), 0.9 (3H, t). ^{13}C NMR ($CDCl_3$): δ/ppm = 151.9, 136.9, 126.3, 110.5, 77.8, 69.4, 53.6, 46.1, 31.9, 31.0, 29.7, 29.4, 26.2, 22.7, 14.1. Elemental analysis (calculated for $C_{28}H_{48}N_2O_3$): %C = 73.25 (73.04), %H = 10.48 (10.43), %N = 6.18 (6.09).

NPOHP. mp = 73−76 °C. FT-IR (KBr): ν/cm^{-1} = 1514, 1479, 1336, 1118. ^{1}H NMR ($CDCl_3$): δ/ppm = 8.1 (2H, d), 6.6 (2H, d), 4.0 (1H, broad), 3.2−3.6 (6H, m), 2.1 (4H, m), 1.5−1.6 (2H, m), 1.2 (26H, br s), 0.9 (3H, t). ^{13}C NMR ($CDCl_3$): δ/ppm = 151.8, 137.0, 126.2, 110.7, 71.7, 70.5, 58.7, 48.6, 31.9, 29.7, 29.4, 28.9, 26.1, 23.2, 22.7, 14.1. Elemental analysis (calculated for $C_{27}H_{46}N_2O_3$): %C = 72.76 (72.65), %H = 10.38 (10.31), %N = 6.32 (6.28).

NPOOP. mp = 78−80 °C. FT-IR (KBr): ν/cm^{-1} = 1514, 1483, 1336, 1118. ^{1}H NMR ($CDCl_3$) : δ/ppm = 8.1 (2H, d), 6.6 (2H, d), 4.0 (1H, broad), 3.2−3.6 (6H, m), 2.1 (4H, m), 1.5−1.6 (2H, m), 1.2 (30H, br s), 0.9 (3H, t). ^{13}C− NMR ($CDCl_3$): δ/ppm = 151.8, 137.2, 126.1, 111.0, 71.8, 70.7, 58.7, 48.6, 31.9, 29.6, 29.4, 28.9, 26.1, 23.2, 22.6, 14.0. Elemental analysis (calculated for $C_{29}H_{50}N_2O_3$): %C = 73.65 (73.42), %H = 10.62 (10.55), %N = 5.98 (5.91).

Samples for the LB experiments were purified by multiple recrystallizations. L-α-distearoylphosphatidylcholine (DSPC) with 99+% purity from Sigma Chemicals was used directly. Crystals of NP3OP and NPOHP were grown from dilute solutions of hexane−dichloromethane and chloroform respectively over a period of 2 days at ∼ 5 °C.

Crystal Structure Determination. X-ray diffraction data were collected on an Enraf-Nonius MACH3 diffractometer. Mo Kα radiation with a graphite crystal monochromator in the incident beam was used. Data were reduced using Xtal3.4;[8] Lorentz and polarization corrections were included. All non-hydrogen atoms were found using the direct method analysis in SHELX-97,[9] and after several cycles of refinement, the positions of the hydrogen atoms were calculated and added to the refinement process. Details of data collection, solution and refinement, fractional coordinates with anisotropic thermal parameters, and full lists of bond lengths and angles are submitted as Supplementary Information.

LB Film Studies. Pressure−area (π−A) isotherms were investigated on a Nima model 611M LB trough (area = 30 × 10 cm^2) using a Wilhelmy plate for sensing surface pressure. High purity water (Millipore MilliQ) was used as the subphase. Chloroform (Uvasol grade, EMerck) solutions (∼1 mM) were spread on the subphase. A 15 min wait period was allowed for solvent evaporation. All experiments were carried out at 25 °C. The π−A isotherms were recorded using a barrier speed of 30 cm^2/min. Experiments were repeated on fresh subphases 2−3 times to confirm reproducibility; the precision of molecular areas extracted is ∼1 Å^2. Area per molecule A_1 is obtained by extrapolation to π = 0 mN/m, of the straight regions of the isotherms just below the plateau representing the flip-over transition (observed above 13 mN/m in all the systems) in the first compression. A_2 is obtained similarly, from the final collapse of the bilayer in the reproducible compressions. The presence of sufficiently long straight regions in the isotherms make this unambiguous in the case of NP3OP and NPOOP; in some of the isotherms of NPOHP, the extrapolated areas would be less accurate because of the limited straight region in the isotherms.

Glass and quartz microscope slides with a hydrophilic surface for the LB film deposition were prepared as follows; high purity water was used in all operations. The substrate was cleaned with detergent followed by several rinsings in water; it was soniccated in fresh lots of water three times for 30 min each. The surface was made hydrophilic by immersing in aqueous sodium hydroxide for 12 h followed by soniccation and rinsing in water. The LB film was coated on both sides of the substrate by the vertical dipping procedure employing a dipping speed of 3 mm/min with the monolayer held at a pressure of 30 mN/m. The specular reflectance (8° incidence) spectrum of the LB film on quartz was recorded on a Shimadzu model UV-3101 UV−visible spectrometer using the integrating sphere (ISR 3100) assembly. The sample as well as the reference uncoated plate were placed with a Teflon sheet at the back. We have chosen to use reflectance over absorption spectra for the LB films because of the improved signal-to-noise ratio obtained. The reflectance spectrum of the solid material was recorded using pellets made from a mixture of the compound and KBr. Absorption spectra of the solutions in hexane were also recorded.

Computational Studies. Semiempirical quantum chemical studies were carried out using the AM1[10] method in the MOPAC93 program package.[11] The microenvironment of the molecule in the condensed phases and the solution phase was simulated using the solvation model COSMO;[12] the utility of this approach has been demonstrated in our earlier studies.[13] The absorption energies and the corresponding transition dipoles were computed from a configuration interaction (CI) calculation on geometries of the molecule and supramolecular assemblies extracted from the crystal structure; the hydrocarbon chains were replaced by methyl groups, and all H atom positions were optimized. The CI calculations invoked the full set of singlet configurations (400) involving 6 molecular orbitals bracketing the HOMO and the LUMO.

Results and Discussion

As noted above regarding several 4-nitroaniline based amphiphiles,[7] NP3OP, NPOHP, and NPOOP do not spread as stable monolayers on the water surface but form visible aggregates. We have therefore explored equimolar mixtures of these systems with cadmium arachidate. In the case of NP3OP, a large hysteresis is observed in the compression−expansion isotherm (isocycle) indicating strong collapse. NPOHP and NPOOP mixtures showed isotherms with a plateau similar to the one observed by Munn and Szczur[7f] for another NPP-based amphiphile mixed with stearic acid. In all of the three cases, the second isocycle was shifted to lower areas. The molecular areas could not be satisfactorily explained on the basis of formation of composite monolayers. Because no consistent model for the mixed monolayers or bilayers could be developed from these observations, we have explored mixtures of these novel amphiphiles with DSPC. Phospholipids form stable monolayers on water and are known to discourage aggregation of guest molecules.[14] Our earlier study of fatty acid-DSPC composites has also suggested its utility as a host matrix.[15]

Equimolar Compositions of NP3OP, NPOHP, and NPOOP with DSPC. We first examined equimolar mixtures of NP3OP, NPOHP, and NPOOP with DSPC on the water surface. The isotherms are presented in Figure 2 parts a−c respectively for NP3OP−DSPC, NPOHP−DSPC, and NPOOP−DSPC; the values plotted on the *x* axis are the mean molecular areas based on the total number of molecules spread on the water surface. The monolayers of the composite systems display complex behavior. In each case, the first isocycle shows plateau formation and hysteresis; subsequent compressions and expansions lead to isocycles which are highly reproducible over extended periods of time but shifted with respect to the first isocycle. Alhough the general patterns are similar, there are significant differences in the details between the three systems. For NP3OP, the second and subsequent isocycles are close to the expansion curve of the first one. In NPOHP−DSPC and NPOOP−DSPC, these are shifted considerably from the first isocycle; reproducibility is achieved from the third and second isocycles, respectively, in the two systems. The shape change between the first and final isocycle is moderate in the NPOHP system but quite dramatic in the case of NP3OP and NPOOP. The values of area/molecule, A_1, at the onset of the plateau (see the Experimental Section for details) are similar in the case of NP3OP−DSPC and NPOOP−DSPC but larger in NPOHP−DSPC. The latter suggests a different orientation of the amphiphile headgroups on the water surface compared to the first two. The extrapolated areas, A_2, from the final collapse of the reproducible compression isotherms in all of the three cases correspond closely to that of a DSPC monolayer as described later. Plateaus in pressure−area isotherms arise as a result of molecular reorientation or chain alignment associated with phase transitions[16] or multilayer formation.[17] The extrapolated areas and the evolution of the isotherm shapes in Figure 2 strongly suggest a "flipping over" of the amphiphiles onto the DSPC monolayer; this would be a natural consequence of the superior stability of DSPC films compared to that of the other amphiphiles. The structure that results is best described as a bilayer as shown by several

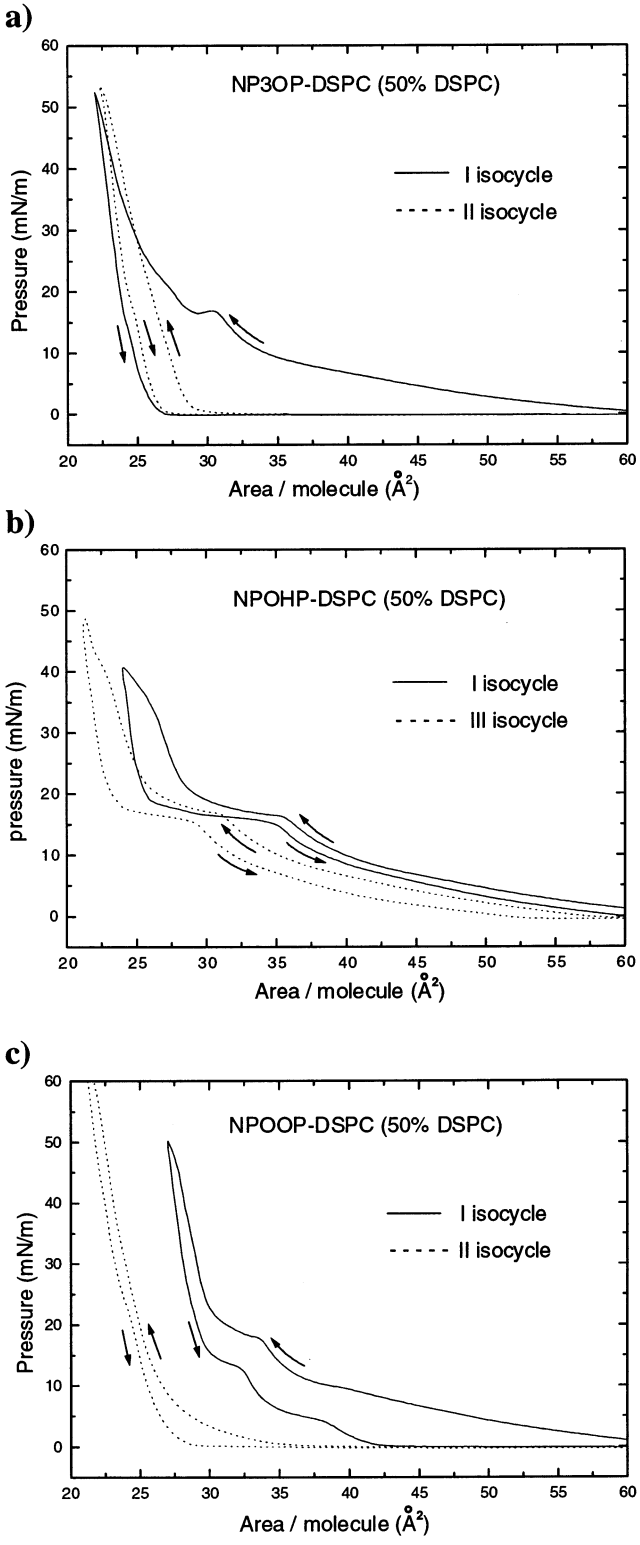

Figure 2. $\pi-A$ isocycles of 1:1 mixtures of (a) NP3OP−DSPC, (b) NPOHP−DSPC, and (c) NPOOP−DSPC; values on *x* axis are the mean molecular areas based on the total number of molecules spread.

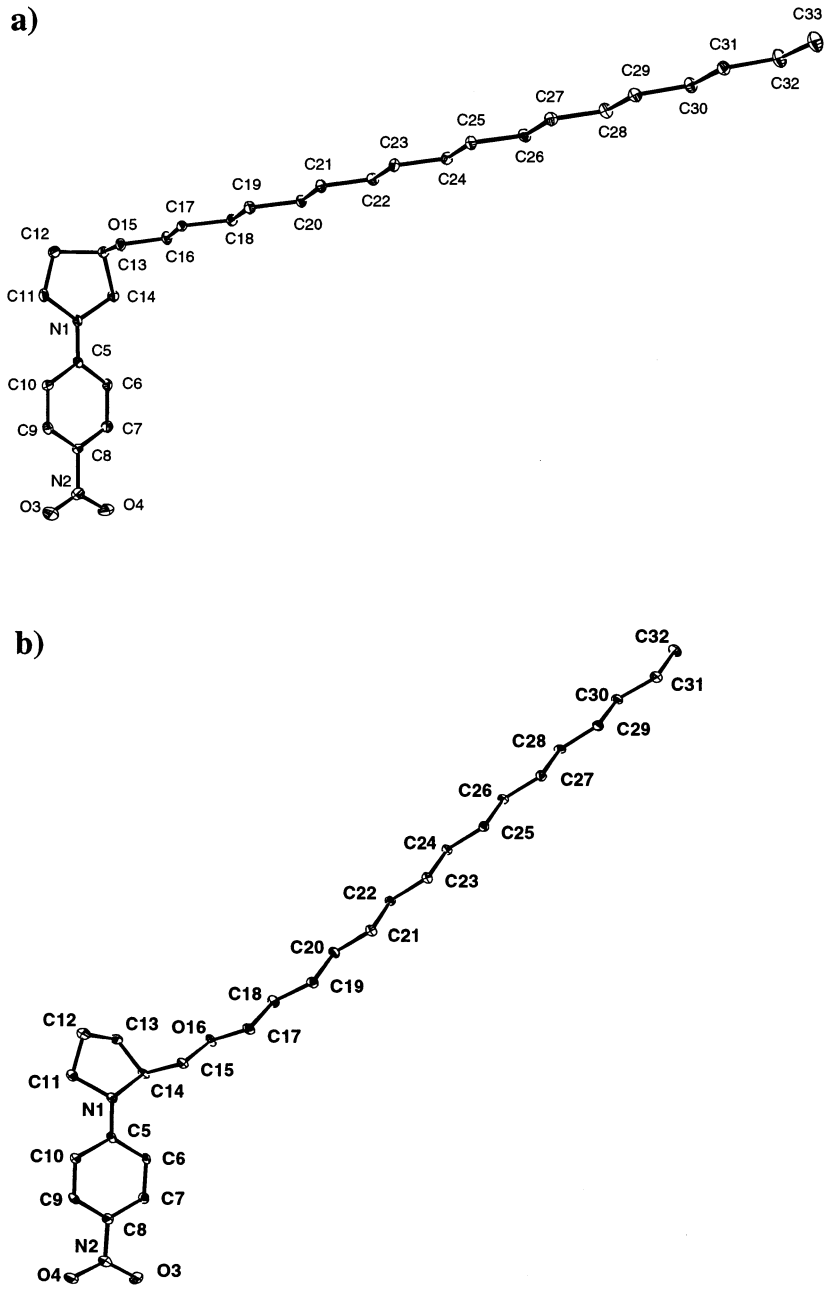

Figure 3. Molecular structure of (a) NP3OP and (b) NPOHP from single-crystal X-ray analysis showing 10% probability thermal ellipsoids.

observations described below. We develop this model and probe the nature of intermolecular interactions in the monolayer and composite bilayer through a unique combination of crystal structure investigations, detailed pressure−area isotherm studies of the mixtures, and electronic absorption spectroscopy of the LB film.

Crystal Structure of NP3OP and NPOHP. We have succeeded in growing single crystals of NP3OP and NPOHP; crystallization of NPOOP was not successful, but the salient features of NPOHP are expected to carry over to NPOOP. The crystallographic data are summarized in Table 1. NP3OP crystallizes in the space group $P2_1$ with one molecule in the asymmetric unit (Figure 3a); the alkyl chain has all-trans conformation. The dihedral angle, τ (C14−C13−O15−C16), that determines the orientation of the alkyl chain with respect to the headgroup is 75.3°. The chain is oriented approximately perpendicular to the dipole axis of the headgroup; the angle between the vector N2−N1 and the vector O15−C33 is 78.6°. Based on the unit cell parameters, the molecular area ($\{ab \sin \gamma\}/2$) of NP3OP is calculated to be 22.0 Å^2; the factor of 2 arises as a result of two molecules sharing the area of the *ab* face (see packing

TABLE 1: Crystallographic Data for NP3OP and NPOHP

	NP3OP	NPOHP
molecular formula	$C_{28}H_{48}N_2O_3$	$C_{27}H_{46}N_2O_3$
formula weight	460.68	446.66
crystal system	monoclinic	orthorhombic
space group	$P2_1$	$P2_12_12_1$
a, Å	8.2829(10)	5.1217(19)
b, Å	5.306(3)	8.7292(17)
c, Å	31.269(5)	59.463(9)
β, deg.	91.897(11)	90
Z	2	4
$\rho_{calc.}$, g cm^{-3}	1.114	1.116
μ, cm^{-1}	0.71	0.72
number of unique reflections	4570	4515
number of reflections with $I \geq \sigma_I$	1874	4154
number of parameters	299	293
GOF	0.983	0.964
R (for I $\geq 2\sigma_I$)	0.0463	0.0598
wR^2	0.1306	0.2336

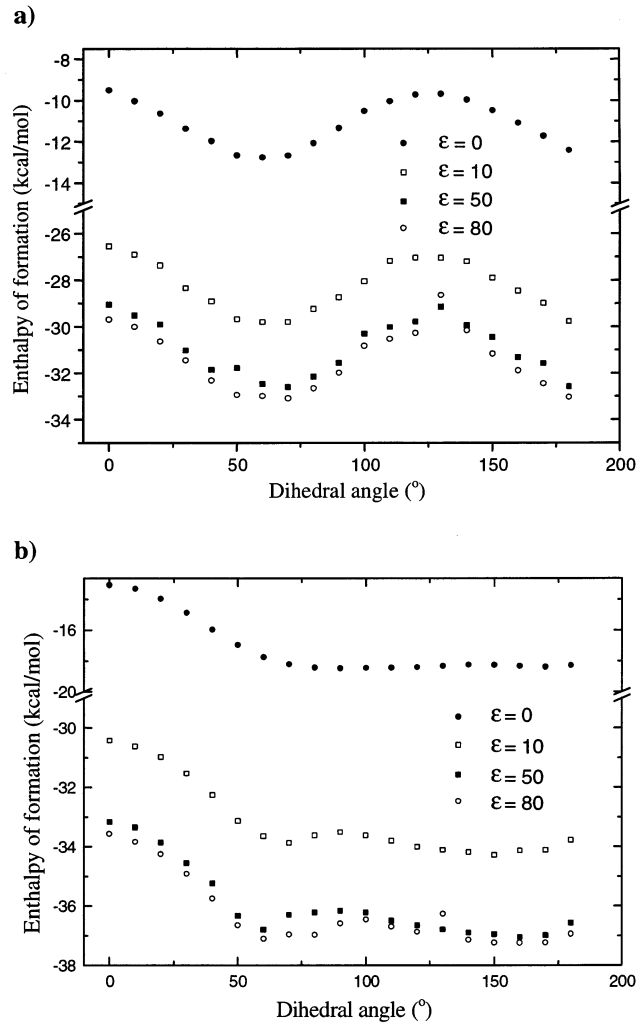

Figure 4. AM1/COSMO calculated enthalpy of formation versus dihedral angle, (a) τ (C14−C13−O15−C16) in NP3MP and (b) τ (N1−C14−C15−O16) in NPOMP for different values of the dielectric constant, ϵ.

diagram later). NPOHP crystallizes in the space group $P2_12_12_1$ with one molecule in the asymmetric unit (Figure 3b); the alkyl chain has an all-trans conformation. The dihedral angle, τ (N1−C14−C15−O16), is 179.7°. This leads to an improved alignment of the alkyl chain with respect to the dipole axis compared to that for NP3OP; the angle between the vector N2−N1 and the vector C15−C32 is 45.0°. The molecular area is estimated to be 22.4 Å^2.

To rationalize the observed τ angles in NP3OP and NPOHP and to estimate the energetics associated with chain reorientations, we have carried out semiempirical AM1 calculations on the model headgroups, NP3MP and NPOMP, in which the alkyl chains of the original molecules are replaced by methyl groups. The crystalline environment was simulated using the solvation model, COSMO. The variation of the enthalpy of formation with τ is shown in Figure 4. In NP3MP, minima are observed near $\tau = 60°$ and 180°. Inclusion of the solvation model with increasing dielectric constants leads to a consistent global minimum at 70°; this is close to the angle observed in the crystal. It is also seen that the barrier to rotation along the τ coordinate is ∼3.5 kcal/mol. Similar computations on NPOMP gives the global minimum at 160°, again in good agreement with the experimental value. The rotational barrier is <1 kcal/mol.

The different orientations of the alkyl chains with respect to the dipole axis in the two molecules (Figure 3) appear to exert a critical influence on their crystal packing (Figure 5); this would also have strong implications for their behavior at the air−water interface[18] as discussed later. The chains are interdigitated in NPOHP. The molecular packing in both crystals takes advantage of the dispersion interaction between the alkyl chains as well as dipole−dipole interactions between the 4-nitroaniline headgroups. The dipole vectors (N2−N1) of neighboring molecules are oriented nearly antiparallel, the angle being 178.5° and 170.7° in NP3OP and NPOHP, respectively. Interestingly, the molecular planes of the headgroups of the near neighbors in both the crystals adopt a nearly orthogonal orientation; the angle between the mean benzene planes of adjacent molecules in NP3OP and NPOHP are respectively 79.6° and 83.1°. Such near neighbor orientations have been observed in crystals of alkyl substituted dipolar chromophores.[19] In the 4-nitroaniline based amphiphiles, this orthogonal orientation appears to be facilitated by a multitude of weak interactions[20] between the nitro group atoms and several atoms on the neighboring molecules. The shortest of the intermolecular contacts observed in NP3OP are O4...C16′ (3.348 Å), O3...C12″ (3.537 Å), N2...C11‴ (3.566 Å), and O3...C11‴ (3.584 Å) and in NPOHP are O3...C11′ (3.246 Å), O3 ...C11″ (3.360 Å), O4...C15‴ (3.394 Å), N2...C11″ (3.402 Å), and N1...O3‴′(3.481 Å) (the primes denote different neighbors of the unprimed molecule). The O....C and N...C represent weak H-bond interactions and the N...O represents the electrostatic interaction. We believe that the push−pull nature of the headgroup enhances the electron density on the nitro group oxygen atoms, improving the strength of these interactions. Such an orthogonal orientation of the push−pull chromophore headgroups which could arise even when the molecular dipoles are oriented parallel (as when spread on a water surface and compressed) would hinder efficient headgroup packing and thwart the formation of stable monolayers of 4-nitroaniline based amphiphiles.

Variable Compositions of NP3OP, NPOHP, and NPOOP with DSPC. In Figure 2a, it is seen that the area, A_1, of the equimolar NP3OP−DSPC system is 38.6 Å^2/molecule and the area A_2 is 28.0 Å^2/molecule. The molecular area of DSPC is ∼54 Å^2.[15,21] Using the molecular area of NP3OP determined from the crystal structure analysis, the mean molecular area for the equimolar composite works out to be 38 Å^2, in good accord with the observed value of A_1. The value of A_2 corresponds closely to the area/molecule of a monolayer of pure DSPC; it should be noted that, because the number of molecules of DSPC is half of the total, the value on the *x* axis should be doubled to calculate the area/molecule with respect to DSPC. The values of A_1 and A_2 are consistent with the proposed model of formation of a composite monolayer of NP3OP and DSPC from which the NP3OP molecules flip over onto the DSPC monolayer at the plateau transition. Such bilayer formations have been reported in earlier studies of composite systems at the air−water interface.[22] The novel and interesting feature in the present case is that on expansion and further compression the isotherm shape changes completely and appears like that of a pure DSPC monolayer exhibiting long-term stability and reproducibility. This indicates that the NP3OP molecules which have flipped over onto the DSPC molecules are retained in some complexed form during expansion and further isocycles. To examine further this model of bilayer formation, we have recorded the $\pi-A$ isotherms of different compositions of NP3OP-DSPC (Figure 6a). The composition of 90% and 10% DSPC are extreme cases, the former behaving nearly like pure DSPC and the latter showing no stable monolayer formation. The extrapolated areas, A_1 and A_2, for the different compositions are presented in Table

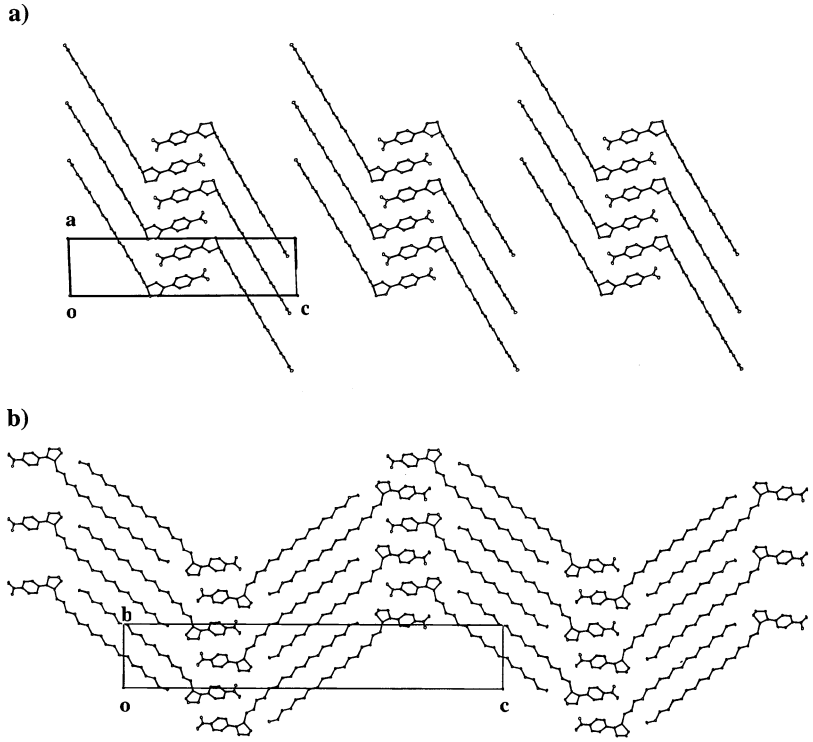

Figure 5. Molecular packing in the crystals of (a) NP3OP and (b) NPOHP.

TABLE 2: Estimated[a] and Observed (Figure 6) Area/Molecule Corresponding to the "Flip-Over" Transition (A_1) and Final Collapse (A_2) for Different Compositions of NP3OP−DSPC, NPOHP−DSPC, and NPOOP−DSPC

		area/molecule (Å^2)					
		NP3OP−DSPC		NPOHP−DSPC		NPOOP−DSPC	
mol % of DSPC	A_1 or A_2	estimate	obsd	estimate	obsd	estimate	obsd
30	A_1	31.6	28.8	54.8	56.2	31.9	34.3
	A_2	25.0	22.6	18.4	19.5	18.4	19.1
40	A_1	34.8	33.1	54.7	59.2	35.0	37.3
	A_2	26.0	25.0	21.6	21.9	21.6	22.4
50	A_1	38.0	38.6	54.6	47.2	38.2	40.0
	A_2	27.0	28.0	27.0	28.5	27.0	26.6
60	A_1	41.2	42.1	54.5	45.0	41.4	40.8
	A_2	32.4	33.1	32.4	36.3	32.4	31.7
70	A_1	44.4	44.1	54.4	*b*	44.5	*b*
	A_2	37.8	37.4	37.8	38.4	37.8	40.3
90	A_1	50.8	*b*	54.1	*b*	50.8	*b*
	A_2	48.6	48.3	48.6	47.8	48.6	47.5

[a] $A_1 = n_{DSPC}A_{DSPC} + n_{NP}A_{NP}$. $A_2 = n_{DSPC}A_{DSPC} + (n_{NP} - xn_{DSPC})A_{NP}$ {for $n_{NP} > xn_{DSPC}$} $= n_{DSPC}A_{DSPC}$ {for $n_{NP} < xn_{DSPC}$}. $A_{DSPC} = 54$ Å^2; A_{NP}, the molecular area for NP3OP, NPOHP, or NPOOP are estimated from crystal structures: NP3OP (22 Å^2), NPOHP (55.2 Å^2 for horizontal 'face-on' orientation and 22.4 Å^2 for vertical orientation, for A_1 and A_2 calculation respectively), NPOOP (22.4 Å^2 from NPOHP); n = mol fraction; $x = 1$ (NP3OP), 2 (NPOHP, NPOOP) (Figure 7). [b] No clear "flip-over" transition observed.

2. The values estimated using the model of NP3OP flipping over (Figure 7a) are also presented in the table. We assume that, under compression conditions, the alkyl chains of NP3OP are reoriented to align with the headgroup axis and that, on flipping over, these molecules relax their chains back to the tilted orientation found in their crystals. This makes them compatible in size with the DSPC molecules, supporting a 1:1 complexation in the bilayer. The A_2 values of the 30% and 40% DSPC mixtures provide critical evidence for this stoichiometry in the bilayer by accounting for the area due to the DSPC layer as well as the unflipped NP3OP. The good agreement between the experimental values and the estimates across the different compositions (Table 2) lends strong support to the "flip-over" model and bilayer formation.

The equimolar NPOHP−DSPC mixture shows an elongated plateau during the first compression (Figure 2b); the value of A_1 is 47.2 Å^2. Because the molecular area of NPOHP determined from the crystal structure is similar to that of NP3OP, the large A_1 suggests that the NPOHP headgroups are tilted toward a horizontal orientation at the air−water interface. This results from a more pronounced hydrophilic headgroup−water interaction because of the shorter length of the alkyl chain of NPOHP and the low energy barrier (Figure 4b) facilitating chain reorientation. The area estimated for the equimolar mixture assuming a horizontal face-on orientation of the headgroup of NPOHP is given in Table 2. Because the observed value is smaller, a tilted orientation of the headgroup is likely. The value of A_2 from the final reproducible isotherms is 28.5 Å^2, closely agreeing with the value for a DSPC monolayer as in the case of NP3OP−DSPC. The plateau of the first compression represents a headgroup reorientation toward the vertical, together with part of the NPOHP molecules flipping over, and the second and third compressions complete the flipping process. The flipping over of the NPOHP molecules appears to be more difficult than that of NP3OP. This is borne out also by the similarity of the shapes between the first and subsequent isocycles of NPOHP−DSPC which suggests partial reversal of the flip-over. A physical interpretation of this behavior is that NPOHP shows a relatively higher affinity to remain on the water surface than NP3OP. The mechanism of chain reorientation on the water surface and relaxation back to the tilted orientation when flipped over onto DSPC promotes the bilayer formation in NP3OP but is altogether absent in the case of NPOHP. The $\pi-A$ curves for the different compositions of NPOHP−DSPC are presented in Figure 6b, and the A_1 and A_2 values are collected in Table 2. In the case of mixtures with less than 50% DSPC, the A_1 values suggest a more horizontal orientation of the headgroups of NPOHP. The A_2 values agree with the estimates assuming two molecules of NPOHP flipping over onto each

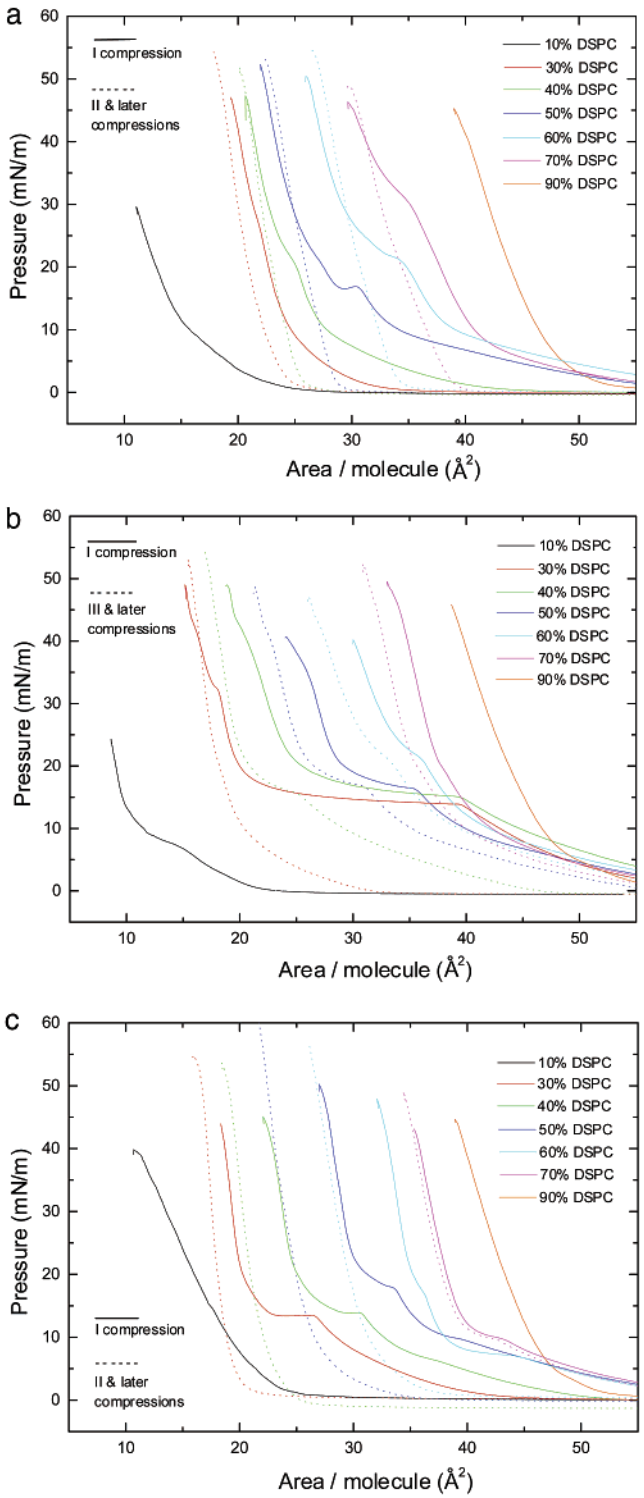

Figure 6. $\pi-A$ isotherms of different compositions of (a) NP3OP−DSPC, (b) NPOHP−DSPC, and (c) NPOOP−DSPC; values on x axis are the mean molecular areas based on the total number of molecules spread.

DSPC to give a 2:1 complex (see Figure 7b). This picture is realistic in view of the better alignment of the chain with the headgroup of NPOHP observed in its crystals. Once again the values of A_2 of the 30% and 40% DSPC systems provide crucial evidence for the stoichiometry. The 30% DSPC system shows a strong change of shape after the first isocycle; the reproducibility observed from the third isocycle onward and its shape suggests that the NPOHP molecules are irreversibly complexed with DSPC and smoothly form the bilayer on compression.

The equimolar NPOOP−DSPC mixture shows a shorter plateau than the one in the case of NPOHP−DSPC during the first compression (Figure 2c); a smooth reorientation of the headgroup is suggested by a minor inflection in the isotherm near 10 mN/m. The value of A_1 is 40.0 Å^2, in good agreement with the value estimated for a monolayer of NPOOP and DSPC. The area of NPOOP is assumed to be 22.4 Å^2, the same as that of NPOHP in the vertical orientation. Unlike NPOHP, the headgroup of NPOOP is oriented vertically at the point of flipping over; this is compatible with the longer alkyl chain of NPOOP. From the second compression onward, the shifted isotherms resemble that of DSPC and are highly reproducible. The value of A_2 is 26.6 Å^2, agreeing very well with the value for a DSPC monolayer. The behavior of NPOOP−DSPC mixtures shows that the flip-over of NPOOP molecules is easier than that of NPOHP but less facile than that of NP3OP. The reasoning for the latter would follow the same logic as in the case of NPOHP, and the former can be attributed to the fact that the longer alkyl chain of NPOOP makes the affinity to water less pronounced than in the case of NPOHP. The $\pi-A$ curves for the different compositions of NPOOP−DSPC are presented in Figure 6c, and the A_1 and A_2 in Table 2 show good agreement with the estimated values; the estimated values of A_2 assume a 2:1 complexation in the bilayer. The behavior largely follows that of NPOHP, but the variations with composition are more systematic because the headgroup reorientation is smooth. At all compositions below 70% DSPC, the final isotherms are very much DSPC-like, indicating irreversible complexation of NPOOP with DSPC. The 70% and 90% DSPC mixtures do not show a clear flip-over transition, but only the inflection due to headgroup reorientation. The flip-over process and bilayer formation required to explain the plateau and area values are schematically represented in Figure 7c.

We have shown that several features of NP3OP, NPOHP, and NPOOP and their composites with DSPC on the water surface can be explained using inputs from the crystal structure of NP3OP and NPOHP. The molecular areas of the composites extracted from the $\pi-A$ isotherms show good correlation with simple additive estimates based on individual molecular areas. Although this could be interpreted as indicative of an immiscible system,[23] the varying plateau pressures across the different compositions (with a clear minimum/maximum in the NP3OP and NPOOP systems, but less systematic in the NPOHP) rule out such a possibility and signify interacting components in the composite monolayer. Further, the collapse pressures are found to vary across the compositions (again more systematic in NP3OP and NPOOP) indicating intermolecular interaction between the nitroaniline amphiphile and DSPC in the bilayer. The flip-over transition demonstrates the dominance of the intermolecular interactions in the bilayer over that in the monolayer. The less well-behaved features of NPOHP compared to NP3OP and NPOOP in all of the cases may be attributed to its shorter chain length. However, its crystal structure provides useful insights into the behavior of NPOOP and explains the critical differences in the behavior of NP3OP with respect to NPOHP and NPOOP in terms of the different chain orientations observed in the crystals. We show further that the molecular level interactions in the LB films of the composite bilayers can be visualized using parallel spectroscopic investigations of the LB films and the crystalline phase.

LB Films. The composite bilayers of equimolar NP3OP−DSPC and NPOOP−DSPC formed after the first isocycle showed good stability. LB films containing up to three layers could be deposited on hydrophilic glass/quartz surfaces. The

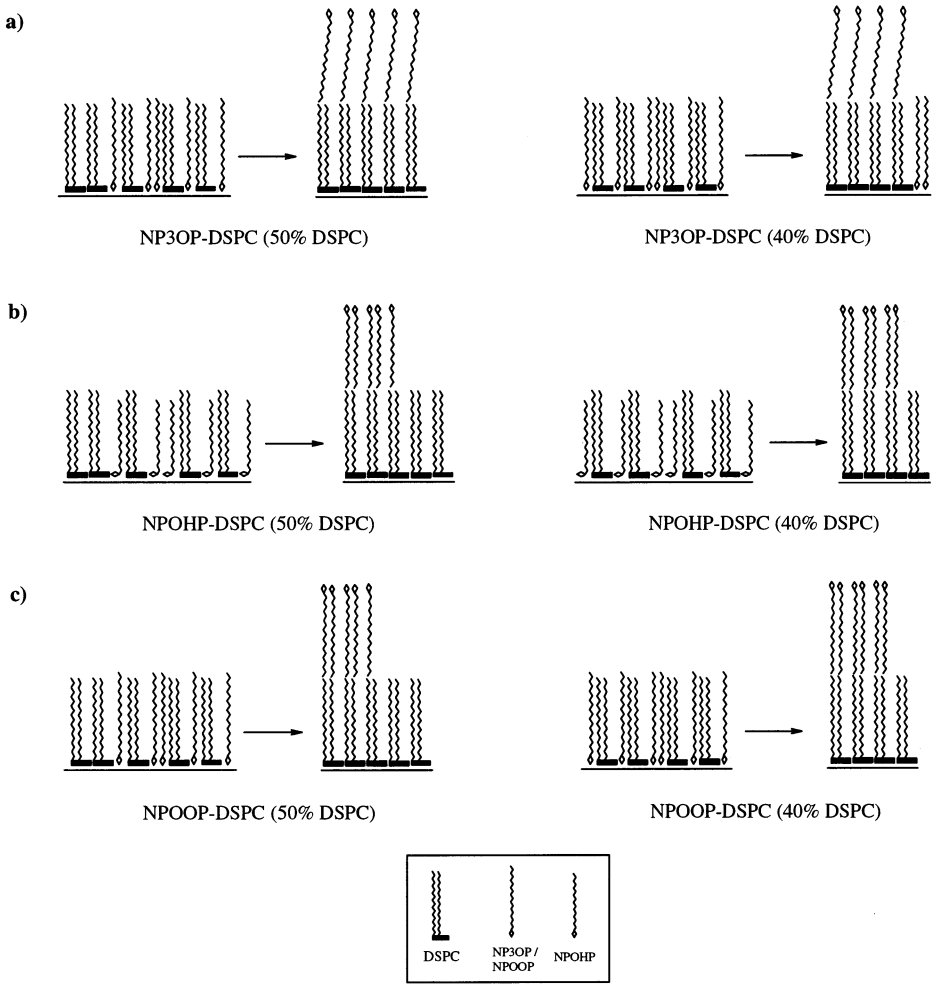

Figure 7. Schematic model of the "flip-over" process and bilayer formation in (a) NP3OP−DSPC, (b) NPOHP−DSPC, and (c) NPOOP−DSPC. Note the horizontal orientation of the headgroup in the case of NPOHP.

transfer ratios were in the range 0.8−1.0. This is noteworthy in view of the fact that phospholipids are generally not amenable to multilayer LB film deposition.[24] The contact angles of water drops on the LB films of the composites were in the vicinity of 70°; this contrasts with the 90° angle observed on monolayer LB films of DSPC. The decreased hydrophobicity of the LB films of NP3OP−DSPC and NPOOP−DSPC is compatible with the picture of bilayer formation presented above (Figure 7). The coated films were characterized using UV−visible reflectance spectra. The spectrum of the NP3OP−DSPC LB films is shown in Figure 8 along with the reflection spectrum of solid NP3OP diluted with KBr and the absorption spectrum of the hexane solution of NP3OP. Because very similar spectra are observed in the case of NPOOP as well, we present a discussion of only the NP3OP system. The additional peaks seen in the LB film and the solid-state spectra compared to those of the solution can be attributed to the electronic excitations of supramolecular assemblies. The relation between the solid-state spectrum and the LB film spectrum supports our earlier interpretation of the monolayer properties using crystal structure information. It also suggests that molecular level interactions in the crystalline material and the LB films are similar. However, some conspicuous differences can be noticed in the broader peaks and additional shoulders in the solid-state spectrum compared to the LB film spectrum. We have carried out semiempirical computations to probe these aspects further.

Energies and transition dipoles were computed for a molecule of NP3MP using the geometry from the crystal structure. The

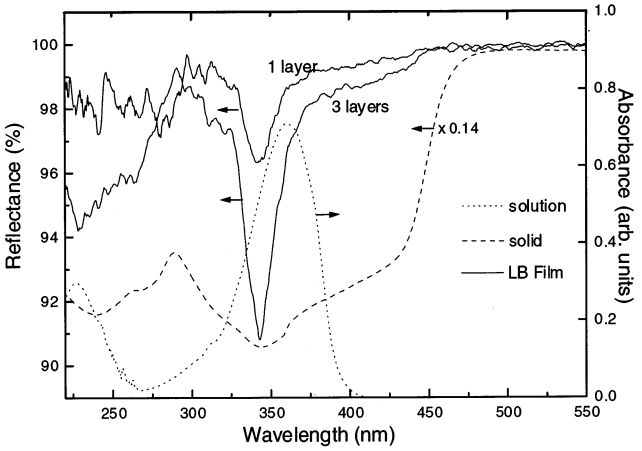

Figure 8. Reflection spectra of LB films of 1:1 NP3OP−DSPC on quartz and the solid pellet of NP3OP (with KBr) and the absorption spectrum of NP3OP in hexane solution.

solvent effect was modeled using the COSMO routine with the dielectric constant value of 2, similar to that of hexane. The strongest peaks computed at 339.2 and 209.7 nm (Table 3) when scaled up by 20 nm match very well with the prominent solution spectral peaks at 360.5 and 226.5 nm. We have computed also the excitation energies and transition dipoles of the monomer and several dimeric, trimeric, tetrameric, pentameric, and heptameric supramolecular fragments of the crystal structure (Figure 9) setting the value of the dielectric constant in the

TABLE 3: Calculated (AM1/CI Including COSMO with $\epsilon = 80$) Absorption Peak Positions and Transition Dipoles for Various Supramolecular Fragments of the Crystals of NP3OP Represented in Figure 9

cluster	peak position (nm) [transition dipole (eÅ)]			
A	368.2 [1.09]	247.8 [0.71]	210.8 [1.01]	
	339.2[a] [1.03]	235.9[a] [0.81]	209.7[a] [1.01]	
B	335.0 [1.56]	312.1 [0.30]	236.3 [0.74]	217.7 [1.05]
C	327.6 [0.82]	261.5 [0.41]	205.5 [0.62]	182.0 [0.25]
D	327.0 [1.84]	290.9 [0.62]	249.6 [0.52]	
E	356.0 [0.30]	326.8 [0.67]	313.8 [2.08]	
F	349.6 [0.91]	341.7 [0.25]	312.9 [1.98]	
G	333.3 [0.33]	315.5 [1.79]	243.4 [0.31]	
H	347.9 [0.41]	335.1 [1.24]	319.2 [1.82]	
I	311.4 [1.22]	241.5 [0.59]		
J	341.4 [0.25]	337.3 [1.83]		
K	291.6 [1.14]			

[a] These values correspond to $\epsilon = 2$ in the COSMO model.

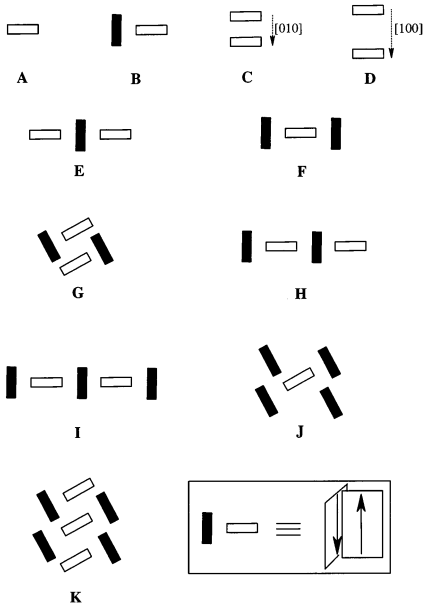

Figure 9. Schematic diagram of molecular clusters of NP3OP used in the AM1/CI calculations. The inset shows the meaning of the symbols used.

solvation model at 80 to mimic the polar environment due to surrounding molecules in the crystal. The computed excitations with wavelengths greater than 180 nm and transition dipoles of at least 0.25 are collected in Table 3. The peaks scaled up by 20 nm are represented schematically in Figure 10a superposed on the absorption spectrum of solid NP3OP obtained using the Kubelka−Munk transformation of the reflectance spectrum in Figure 8. The calculated peaks satisfactorily explain a major part of the observed spectrum and indicate that the observed peaks arise because of the electronic excitations in various groups of molecules that can be envisioned in the crystal lattice. Despite exploring a wide range of further clusters, no calculated excitations were found in the region above 400 nm. The peak

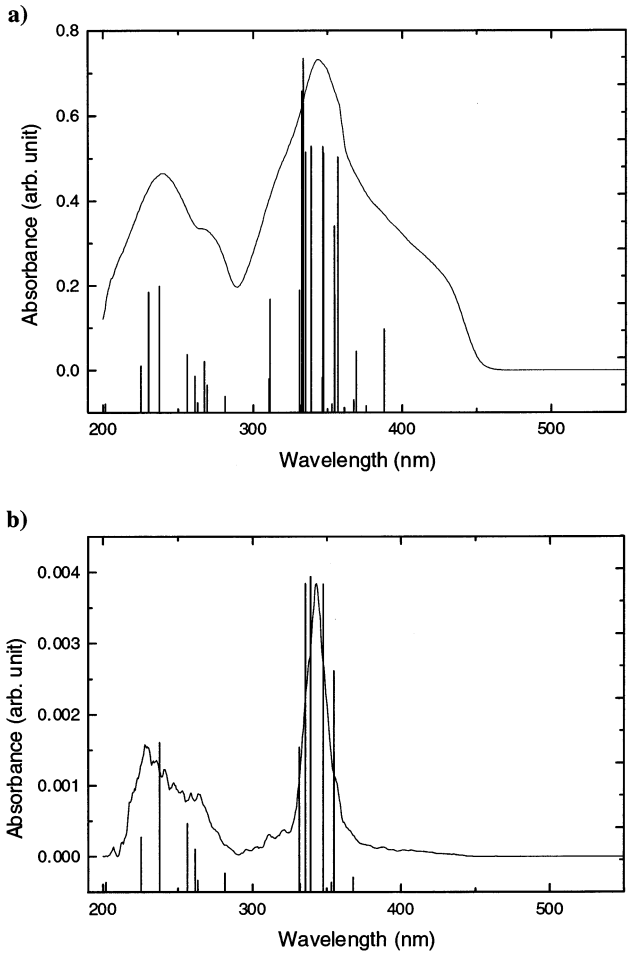

Figure 10. Absorption spectrum (Kubelka−Munk transformation of the reflectance spectrum in Figure 8) of (a) solid NP3OP and (b) 3-layer LB film of 1:1 NP3OP−DSPC. The vertical lines represent the AM1/CI calculated absorption peaks for the clusters shown in Figure 9; the intensities are proportional to the product of the excitation energy and the square of the transition dipole or the oscillator strength.

observed in this region of the solid-state spectrum appears to result from some kind of a J-aggregate structure which may not be a part of the periodic crystal lattice. The Kubelka−Munk transformed spectrum of the three-layer LB film is shown in Figure 10b. All of the prominent features in the spectrum are accounted for using selected clusters (B, C, D, E) from the set in Figure 9. Clearly, a subset of small fragments picked from the 3-dimensional crystal lattice, represent satisfactorily the interacting molecules in the quasi-2-dimensional LB film. Taking into account the possibility that LB films often exhibit microheterogeneous morphology, the present study shows that the crystal structure provides a useful basis to analyze the average nature of molecular associations and interactions in the LB film.

Conclusion

We have presented in this paper a combination of crystallographic investigations and Langmuir/LB film studies of new amphiphiles based on the 4-nitroaniline moiety of interest in quadratic NLO applications. The crystal structure provided insight into molecular level interactions that possibly hamper stable monolayer formation of 4-nitroaniline-based amphiphiles in general. The orthogonal orientation of the 4-nitroaniline groups observed in the crystals is likely to make it difficult for the headgroups of the amphiphiles to arrange in eclipsed or

slipped parallel π stacks to develop into extended monolayers. We have demonstrated the utility of DSPC monolayers in accommodating these amphiphiles in a composite bilayer motif. The crystallographic characterization of the amphiphilic molecules enabled us to develop a viable model for the complex pressure−area isotherms of the composite monolayers containing the amphiphiles. The electronic absorption spectrum together with the computational modeling leads to a picture of the average intermolecular interactions between the push−pull chromophore units in the LB films in terms of supramolecular fragments of the crystal.

This study provides a systematic demonstration of the correlation between 2-dimensional or quasi-2-dimensional Langmuir/LB films and 3-dimensional crystal lattice. We have carried out similar crystallographic and LB film studies on *N*-octadecyl-2,4-dinitroaniline and *N*-octadecyl-*N*-(4-nitrophenyl)-4-nitroaniline which shows that the approach presented in this paper can be extended to more systems. Further characterizations of the LB films and nonlinear optical studies are under way.

Acknowledgment. Financial support from the Department of Science and Technology, New Delhi (Swarnajayanti Fellowship), the use of the National Single Crystal Diffractometer Facility funded by the DST at the School of Chemistry, University of Hyderabad and technical support from Nima Technology, U.K. are gratefully acknowledged. S.S. thanks the CSIR for a senior research fellowship. We thank Dr. N. M. Rao (Center for Cellular and Molecular Biology, Hyderabad) and Dr. M. J. Swamy for fruitful discussions and valuable suggestions.

Supporting Information Available: Synthesis details of NP3OP, NPOHP, and NPOOP, full crystallographic data on NP3OP and NPOHP, computational results on the molecular clusters, and summary of crystallographic database search (18 pages). This material is available free of charge via the Internet at http://pubs.acs.org.

References and Notes

(1) (a) Roberts, G. *Langmuir- Blodgett Films*; Plenum Press: New York, 1990. (b) Tredgold, R. H. *Order in Thin Organic films*; Cambridge University Press: Cambridge, 1994. (c) Petty, M. C. *Langmuir- Blodgett Films − An Introduction*; Cambridge University Press: Cambridge, 1996.

(2) Cambridge Structural Database, version 5.21.

(3) Yam, M. W.; Lau, V. C.; Wang, K.; Cheung, K.; Huang, C. *J. Mater. Chem.* **1998**, *8*, 89.

(4) Zyss, J.; Nicoud, J. F.; Coquillay, M. *J. Chem. Phys.* **1984**, *81*, 4160.

(5) Oudar, J. L.; Hierle, R. *J. Appl. Phys.* **1977**, *48*, 2699.

(6) (a) Moran, A. M.; Kelley, A. M. *J. Chem. Phys.* **2001**, *115*, 912. (b) Mansour, G.; Creedon, W.; Dorrestein, P. C.; Maxka, J.; MacDonald, J. C.; Helburn, R. *J. Org. Chem.* **2001**, *66*, 4050. (c) Gangopadhyay, P.; Radhakrishnan, T. P. *Angew. Chem., Int. Ed.* **2001**, *40*, 2451.

(7) (a) Inoue, T.; Yase, K.; Okada, M.; Okada, S.; Matsuda, H.; Nakanishi, H.; Kato, M. *Jpn. J. Appl. Phys.* **1988**, *27*, 1635. (b) Miyamoto, Y.; Kaifu, K.; Saito, M.; Kato, M.; Kawamura, K. *Thin Solid Films* **1989**, *178*, 493. (c) Decher, G.; Tieke, B.; Bosshard, C.; Günter, P. *Ferroelectrics* **1989**, *91*, 193. (d) Shin, D.; Park, M.; Lim, S. *Thin Solid Films* **1998**, *327−329*, 607. (e) Nalwa, H. S.; Watanabe, T.; Ogino, K.; Sato, H.; Miyata, S. *J. Mater. Sci.* **1998**, *33*, 3699. (f) Munn, R. W.; Szczur, O. *Mol. Cryst. Liq. Cryst.* **2001**, *355*, 305.

(8) *Xtal3.4*; Hall, S. R., King, G. S. D., Stewart J. M., Eds.; University of Western Australia: Perth, Australia, 1995.

(9) *SHELX-97*, Sheldrick, G. M., University of Göttingen: Göttingen, Germany, 1997.

(10) Dewar, M. J. S.; Zoebisch, E. G.; Healy, E. F.; Stewart, J. J. P. *J. Am. Chem. Soc.* **1985**, *107*, 3902.

(11) MOPAC93; Fujitsu Inc.

(12) Klamt, A.; Shüürmann, G. *Perkin Trans.* **1993**, 799.

(13) (a) Sharma, S.; Radhakrishnan, T. P.; *J. Phys. Chem. B* **2000**, *104*, 10191. (b) Jayanty, S.; Radhakrishnan, T. P.; *Chem. Mater.* **2001**, *13*, 2460l. (c) Sharma, S.; Sharat Chandra, M.; Radhakrishnan, T. P. *Langmuir* **2001**, *17*, 8118.

(14) Gust, D.; Moore, T. A.; Moore, A. L.; Luttrull, D. K.; DeGraziano, J. M.; Boldt, N. J.; Van der Auwerar, M.; De Schryver, F. C. *Langmuir* **1991**, *7*, 1483.

(15) Sharma, S.; Radhakrishnan, T. P. *Thin Solid Films*, **2001**, *382*, 246.

(16) (a) Vogel, V.; Möbius, D. *Thin Solid Films* **1985**, *132*, 205. (b) McConnell, H. M. *Annu. Rev. Phys. Chem.* **1991**, *42*, 171. (c) Hwang, J.; Tamm, L. K.; Böhm, C.; Ramalingam, T. S.; Betzig, E.; Edidin, M. *Science* **1995**, *270*, 610. (d) Schwartz, D. K. *Surf. Sci. Rep.* **1997**, *27*, 241. (e) Ashwell, G. J.; Leeson, P.; Bahra, G. S.; Brown, C. R. *J. Opt. Soc. Am. B* **1998**, *15*, 484. (f) Overs, M.; Fix, M.; Jacobi, S.; Chi, L. F.; Sieber, M.; Schäfer, H. F.; Fuchs, H.; Galla, H. J. *Langmuir*, **2000**, *16*, 1141.

(17) (a) Barraud, A.; Flörsheimer, M.; Möhwald, H.; Richard, J.; Ruaudel-Teixier, A.; Vandevyver, M. *J. Colloid Interface Sci.* **1988**, *121*, 491. (b) Lavigne, P.; Tancrède, P.; Lamarche, F.; Grandbois, M.; Salesse, C. *Thin Solid Films* **1994**, *242*, 229. (c) Goldenberg, L. M.; Becker, J. Y.; Levi, O. P.; Khodorkovsky, V. Y.; Shapiro, L. M.; Bryce, M. R.; Cresswell, J. P.; Petty, M. C. *J. Mater. Chem.* **1997**, *7*, 901.

(18) Okuyama, K.; Watanabe, H.; Shimomura, M.; Hirabayashi, K.; Kunitake, T.; Kajiyama, T.; Yasuoka, N. *Bull. Chem. Soc. Jpn.* **1986**, *59*, 3351.

(19) (a) Gangopadhyay, P.; Sharma, S.; Rao, A. J.; Rao, D. N.; Cohen, S.; Agranat, I.; Radhakrishnan, T. P. *Chem. Mater.* **1999**, *11*, 466. (b) Gangopadhyay, P.; Rao, S. V.; Rao, D. N.; Radhakrishnan, T. P. *J. Mater. Chem.* **1999**, *9*, 1699. (c) Sharma, S.; Radhakrishnan, T. P. *Mol. Cryst. Liq. Cryst.* **2000**, *338*, 257.

(20) Desiraju, G. R. *Acc. Chem. Res.* **1996**, *29*, 441.

(21) Bos, M. A.; Nylander, T. *Langmuir* **1996**, *12*, 2791.

(22) (a)Kawabata, Y.; Sekiguchi, T.; Tanaka, M.; Nakamura, T.; Komizu, H.; Honda, K.; Manda, E. *J. Am. Chem. Soc.* **1985**, *107*, 5270. (b) Kurata, T.; Tsumura, A.; Fuchigami, H.; Koezuka, H. *J. Phys. Chem.* **1991**, *95*, 8831.

(23) Dynarowicz-Łątka, P.; Kita, K. *Adv. Colloid Interface Sci.* **1999**, *79*, 1.

(24) Girard-Egrot, A. P.; Morélis, R. M.; Coulet, P. R. *Langmuir* **1996**, *12*, 778.